Research Article

Journal of Environmental Nanotechnology

Performance and Emission Analysis of a Single-cylinder Diesel Engine Fueled with Nanoparticle-dispersed Biodiesel Blends

Tallapureddy Subba Reddy[1], Juluru Pavanu Sai[2*], Suneel Donthamsetty[3], Doris Ifeoma Ogueri[4] and P. V. Elumalai[5,6]

[1]Department of Mechanical Engineering, Andhra Loyola Institute of Engineering and Technology, Vijayawada, AP, India
[2]Department of CSE Allied Branches, VIKAS College of Engineering and Technology, Nunna, AP, India
[3]Department of Mechanical Engineering, Narasaraopeta Engineering College, Narasaraopeta, AP, India
[4]Department of Faculty Management, Shinawatra University, Pathum Thani, Thailand
[5]Department of Mechanical Engineering, Aditya University, Surampalem, India
[6]Research Fellow, INTI International University, Malaysia
Received: 14.01.2026 Accepted: 16.02.2026 Published: 30.03.2026
*subbuvenky693@aliet.ac.in

ABSTRACT

The study investigates the potential of biodiesel as an alternative fuel to conventional diesel. Biodiesel, produced from vegetable oil through transesterification, offers a more sustainable and environmentally friendly option. While biodiesel shares similar physical and chemical properties with mineral diesel, modifications are necessary for optimal engine performance. This research focuses on developing biodiesel from groundnut oil and optimizing the transesterification process. Characterization of the produced biodiesel showed properties comparable to mineral diesel. Engine tests demonstrated improved performance with biodiesel. Additionally, the incorporation of nanoparticles into the biodiesel blend enhanced the performance and combustion characteristics, offering a promising solution for reducing fossil fuel dependence and environmental impact.

Keywords: CI engine; Biodiesel; Nanoparticles; Transesterification; Energy efficiency.

1. INTRODUCTION

Fossil fuels have historically been fundamental in powering engines for electricity generation and domestic use (Junshuai *et al.* 2022). However, the combustion of these fuels, along with increasing use of automobiles, has led to severe environmental consequences. The release of unburnt hydrocarbons, carbon monoxide and nitrogen oxides contributes significantly to air pollution and climate change by trapping heat (Tao *et al.* 2021). The finite nature of fossil fuels, combined with their unstable prices due to rising demand for power generation and transportation, exacerbates these issues (Venkatesan *et al.* 2017).

In response to the environmental and economic challenges posed by fossil fuels, there is a growing emphasis on promoting low-carbon living and exploring clean, sustainable energy sources. The current global scenario of fossil fuel depletion, rising fuel prices, and associated environmental contamination emphasize the need for alternative fuels (Venkatesan *et al.* 2017). Consequently, researchers are focused on identifying renewable energy sources that are technically viable, readily available, and globally suitable. This search is driven not only by the depletion of fossil fuels but also by the urgent need to address the environmental crisis resulting from their combustion (Manzoore *et al.* 2020; Manzoore *et al.* 2018).

In the current context, research into alternative fuels is justified as it promises overall development in sustainable energy resources, environmental improvement, and establishment of a sustainable fuel life cycle M, P., (Zhang *et al*. 2025). Bio-origin fuels, such as those derived from plants and animal fats, are viable alternatives to address the global petroleum crisis.

(Habibullah *et al.* 2014) examined palm and coconut oil methyl ester blends and found that while they produced low brake torque and high brake specific fuel consumption, they also reduced HC, CO, and smoke emissions. Notably, combined palm and coconut oil blends outperformed individual biodiesel blends in terms of both performance and emissions.

(Erkan, 2015) studied cananol-hazelnut soapstock biodiesel and observed reduced ignition delay and maximum heat release rates with biodiesel addition. However, higher biodiesel blends led to deteriorated combustion due to increased density, viscosity, and surface tension, resulting in higher HC, CO, and smoke emissions and lower NO_x emissions.

Edible oils like coconut and sunflower have been successfully converted into biodiesel, and their blends with fossil diesel have demonstrated improved emission characteristics. Other vegetable oils, such as groundnut and gingelly, have also been used to produce biodiesel for CI engine applications (Patil *et al.* 2009; Kalam *et al.* 2003; Dueso *et al.* 2018).

Studies have shown that direct and indirect injection of coconut oil into diesel engines can yield positive results, including reduced smoke and NO_x emissions. However, the use of pure coconut oil can negatively impact engine performance by decreasing brake mean effective pressure and increasing brake specific fuel consumption (Machacon *et al.* 2001a; Machacon *et al.* 2001b). To mitigate these issues, lower concentrations of pure oil and the addition of alcohols to improve atomization and reduce viscosity can be explored.

Overall, by harnessing renewable resources, biofuels can play a crucial role in achieving a more sustainable and environmentally friendly energy landscape (Mohadesi *et al.* 2014).

Nanoparticle-dispersed biodiesel blends have shown promising results in enhancing the performance and combustion characteristics of single-cylinder diesel engines. Studies utilizing various nanoparticles such as aluminium oxide, zinc oxide, and graphene oxide in biodiesel blends have demonstrated improvements in brake thermal efficiency (BTE), brake-specific fuel consumption (BSFC), combustion pressure, noise emissions, and reductions in emissions like hydrocarbons, carbon monoxide, and nitrogen oxides. Addition of aluminium oxide nanoparticles to JB30 and mahua biodiesel blends resulted in increased BTE, reduced BSFC, and lowered emissions (Tao *et al.* 2021; Venkatesan *et al.* 2017). Similarly, the incorporation of zinc oxide nanoparticles in rice bran biodiesel blends led to enhanced BTE, BSFC, and exhaust emission reductions (Manzoore *et al.* 2020). These findings highlight the potential of nanoparticle-dispersed biodiesel blends to optimize engine performance and reduce emissions, demonstrating a promising avenue for sustainable fuel alternatives.

The process of conversion of straight vegetable oils (SVOs) to biodiesel can be a process using four different technologies namely, heating/pyrolysis, dilution/blending, micro-emulsion and transesterification. Among all these techniques, transesterification is easy, fast and most promising process for the reduction of viscosity and density of SVOs.

2. MATERIALS AND METHODOLOGY

In the current work, used vegetable oil, prepared through a two-stage transesterification process along with diesel and copper chloride ($CuCl_2$) nanoparticles as additives was employed in a four-stroke, water-cooled, single-cylinder, naturally aspirated, direct injection engine with a rated power of 3.5 KW at 1500 rpm.

2.1 Procedure for Acid-catalyzed Transesterification

Used vegetable oil was transformed into biodiesel through base-catalyzed transesterification process using methanol/potassium hydroxide (KOH) as a catalyst. Initially, the oil was filtered to remove impurities before being heated to accelerate the subsequent reaction. A mixture of the heated oil, methanol, and KOH was prepared in a conical flask and subjected to continuous heating and stirring using a magnetic stirrer hot plate. The reaction temperature was maintained at 60°C for an hour, followed by cooling to room temperature for approximately 8-10 hours to allow for phase separation. The biodiesel and glycerol layers were separated using a separating funnel. Finally, the biodiesel was purified by washing with water at 90°C while stirring.

2.1.1 Sonication

Sonication was carried out by exposing the liquid to high frequency ultrasonic waves. The alternating low- and high-pressure cycles generated cavitation bubbles within the liquid. These bubbles expanded during the low-pressure phase and collapsed violently during the high-pressure phase, producing localized shock waves, high temperatures, and intense shear forces. The resulting energy broke molecular interactions, reduced particle size, deagglomerated clustered particles, and enhanced mixing. This process ensured efficient dispersion of nanoparticles, improved homogeneity of the solution, and stabilization of emulsions.

2.2 Nanoparticles as Fuel Additives

Metal-based nanoparticles have emerged as promising additives for diesel and biodiesel fuels. By acting as combustion catalysts, these nanoparticles can enhance fuel properties, mitigate incomplete combustion, and reduce harmful exhaust emissions. The catalytic effect of these additives accelerates combustion, leading to improved fuel economy and lower emissions.

Commonly used metal-based additives include cerium, iron, platinum, and their combinations, as well as other metals like manganese, barium, calcium, and copper. In the context of biodiesel, nanoparticles such as

CuO, $CuCl_2$, $CoCl_2$, $FeCl_3$, and $CuSO_4$ have shown potential as fuel-borne catalysts (FBCs).

The incorporation of FBCs into biodiesel has demonstrated significant improvements in engine performance metrics, including brake power (BP) and specific fuel consumption (SFC). These enhancements are attributed to increased cylinder gas pressure and heat release rates, coupled with reduced ignition delay under optimal operating conditions. In the present study, $CuCl_2$ nanoparticles were employed as additives.

2.3 Synthesis of Nanoparticles

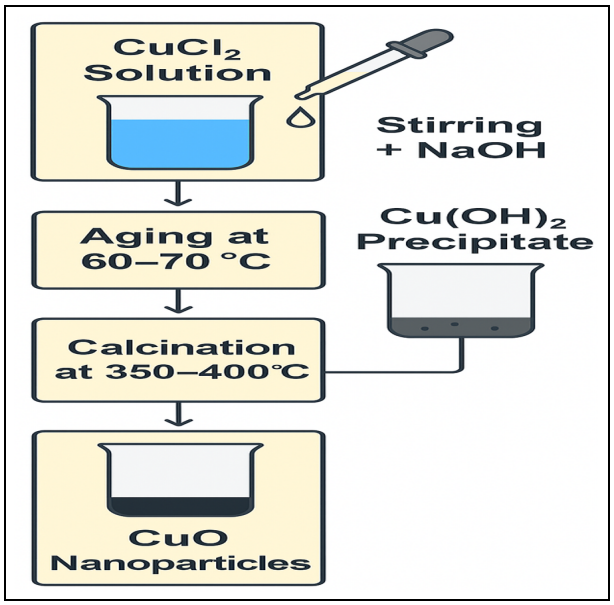


Fig. 1: Synthesis of Nanoparticles

Copper (II) chloride dihydrate was dissolved in distilled water to make a 0.05 M solution and polyvinylpyrrolidone was added to the solution. Polyvinylpyrrolidone acts as a stabilizing agent to prevent agglomeration. Sodium hydroxide solution (0.2 M) was added dropwise with stirring until the pH became 12, causing copper hydroxide to precipitate. The suspension was kept at about 60–70 °C for one hour. The resulting black solid was then washed with distilled water and ethanol for several times and centrifuged to remove chloride and sodium ions. The obtained material was then dried overnight at 60 °C and calcined at the temperature of 350 °C - 400 °C for 2 hours to produce pure and well-crystallized CuO nanoparticles. These were gently crushed and placed in air-tight jars for further characterization and application (Fig. 1).

2.4 Fuel Preparation

To have a uniform and stable dispersion of CuO nanoparticles into the fuel, the fuel with 250 mg of CuO nanoparticles was subjected to ultrasonication. First, a small amount of the nanoparticles underwent mixing with a minor quantity of ethanol, and a stabilizer was employed to avoid agglomeration. The mixture was then subjected to probe ultrasonication (a high-frequency sound waves technique that produces cavitation bubbles through the rapid collapse of gas-filled bubbles), releasing energy to destroy clusters of aggregated particles. The prepared fine suspension was added slowly to the base fuel while stirring to ensure uniformity. For better homogeneity, the blended fuel underwent bath ultrasonication so that the nanomaterials could be distributed uniformly in liquid medium. The spacing between solid nanoparticles and nano-fuel prevents clumping over long term storage. They were stored in air tight containers (without light and air) and bubbled once in a while to keep them from settling to the bottom, just to ensure stability before use. Ultrasonication was the key in producing a well-separated and homogenous fuel blend, with no visible sedimentation.

3. EXPERIMENTAL SETUP

The experimental investigation was conducted using a single-cylinder, four-stroke, naturally aspirated, water-cooled, direct injection diesel engine rated at 3.5 kW at 1500 rpm. Engine specifications are provided in Table 1. The experimental setup comprised of an engine coupled to an eddy current dynamometer, fuel and air supply systems, a water-cooling system, an emission analyzer, a smoke meter, an exhaust gas calorimeter, a computer system, an in-cylinder pressure sensor, thermocouples, and a data acquisition (DAQ) system. The pressure transducer signal was amplified using a charge amplifier. The engine load was controlled through the eddy current dynamometer while maintaining a constant speed of 1500 rpm.

Fig. 2 shows a pictorial representation of the complete experimental test rig, including engine control systems, smoke meter, gas analyzer, and computer system with Enginsoft. This software facilitated comprehensive analysis and visualization of performance and combustion parameters for each fuel blend. Experiments were conducted at four different load conditions for diesel, B20, B20+40 ppm, and B20+80 ppm fuel blends.

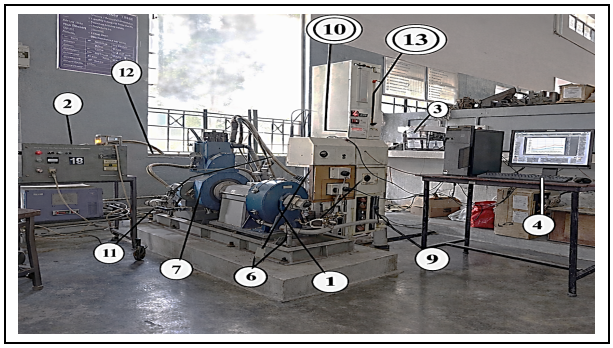


Fig. 2 Separator and its components

Components: 1: Eddy current dynamometer; 2: AVL 437 Smoke Meter; 3: AVL 444 Gas Analyzer; 4: Computer system; 5: Panel Board; 6: Loading Unit; 7: Engine; 8: Fuel Measuring Unit; 9: Coolant Flow Meter; 10: Temperature Indicator; 11: Air-Inlet; 12: Smoke Exhaust; 13: RPM Indicator

Table 1. Engine specification

S. No.	Item	Specifications
1.	Type	Single cylinder, 4 Stroke, Vertical Diesel
2.	Made	Kirloskar Engine, Pune, India
3.	Speed	1500 rpm
4.	Rated Power	3.5 kW
5.	Bore	87.5 mm
6.	Compression Ratio	12:1 to 20:1
7.	Stroke Length	110 mm
8.	Fuel	Diesel
9.	Type of Cooling	Water Cooled
10.	Type of Loading	Eddy Current Dynamometer
11.	Arm Length	155 mm

4. MATHEMATICAL MODEL

The following formulae were employed to determine engine performance parameters:

Brake power was calculated using the equation (1)

$$BP = \frac{(2\,\pi\,N\,T)}{60} \quad \ldots (1),$$

Where, N = Engine Speed in rpm

T = Torque

T = WR

W = Load acted on the engine

R = The dynamometer arm radius (constant at 0.24 m)

Fuel consumption (FC) was calculated using equation (2)

FC = (V * density of water) / (t * Specific gravity of fuel)… (2),

where V = Fuel volume (constant at 10 CC)

t = FC time in seconds

Density of water = 1000 Kg/m^3

Calculated BTE using equation (3)

$$BTE = (FP / BP) * 100 \quad \ldots (3),$$

where BP = Brake power (KW)

FP = Fuel Power (KW)

Specific Fuel Consumption is a standardized metric that quantifies an engine's fuel efficiency by measuring the amount of fuel consumed to produce a unit of power. It is calculated by dividing the fuel consumption rate by the generated power output. Unlike raw fuel consumption values, SFC enables a direct comparison of fuel efficiency between engines of different sizes.

5. ENGINE PERFORMANCE EVALUATION

5.1 Variation of Brake Thermal Efficiency with Engine Load

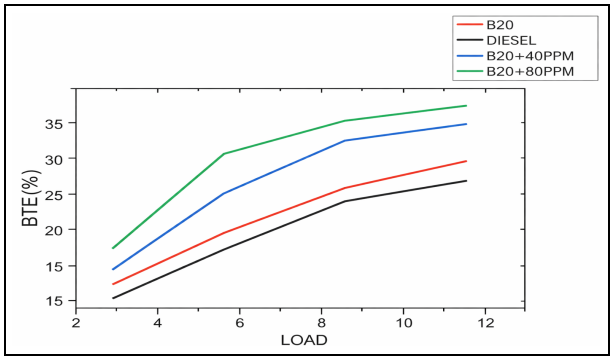


Fig. 3: Variation of BTE with engine load for different fuel blends

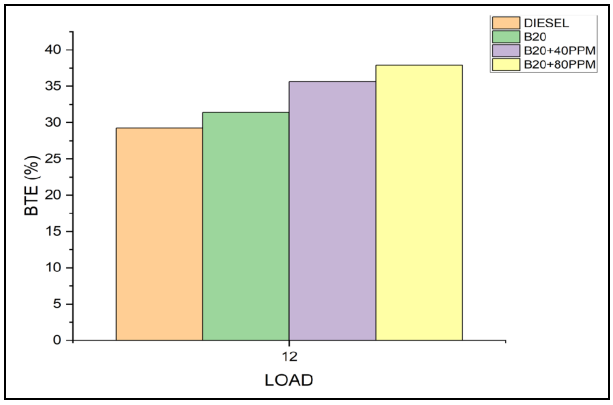


Fig. 4: Variation of BTE with 12 kg engine load for different fuel blends

Nanoparticle-diesel blends exhibited a slight increase in BTE compared to pure diesel operation (Fig. 3). However, biodiesel and its blends demonstrated a decrease in BTE relative to diesel. This reduction is primarily attributed to the lower calorific value of biodiesel compared to diesel. As the biodiesel content in diesel-biodiesel blends increased, the overall calorific value of the fuel blend decreased linearly (Munimathan *et. al* 2025).

Furthermore, while biodiesel blends shortened ignition delay, they also resulted in increased combustion duration. This interplay of factors influenced the overall engine performance and emissions characteristics (Sabri *et al.* 2026)

Fig. 4 shows that all fuel blends exhibited improved BTE under maximum load conditions. A direct correlation was observed between increased load and enhanced efficiency. The B20+80 ppm blend demonstrated the most significant efficiency gains, indicating its potential to optimize engine performance while reducing fuel consumption.

5.2 Variation of Brake Specific Fuel Consumption with Load

Brake thermal efficiency and brake specific fuel consumption are inversely related. An increase in BTE corresponds to a decrease in BSFC, indicating improved fuel efficiency.

At lower engine loads, BSFC tends to be higher due to less efficient combustion and increased frictional losses relative to power output. As the engine load increases, combustion efficiency improves, leading to a reduction in BSFC.

The lower heating value of biodiesel blends compared to diesel results in higher BSFC values for diesel and different fuel blends (Fig. 5). This relationship is evident across different load conditions. At lower loads, the detrimental effect of low heating value on BSFC is more pronounced.

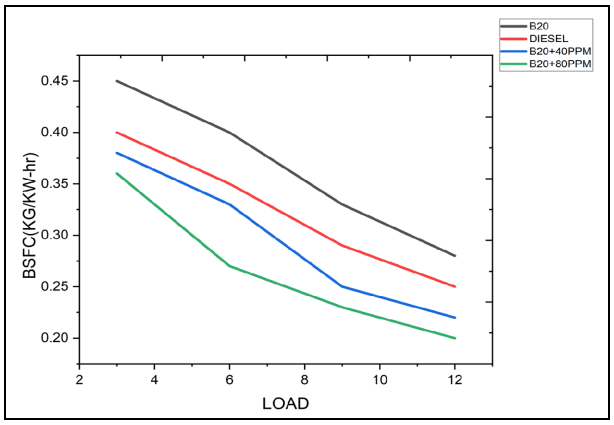


Fig. 5: Variation of BSFC with engine load for different fuel blends

An experimental investigation was conducted to assess the BSFC of diesel and different fuel blends across varying engine loads from 3 kg to 12 kg (Fig. 6). The results indicated a consistent trend of decreasing BSFC with increasing engine load for all fuel types. This implies improved fuel efficiency at higher load conditions for both diesel and biodiesel blends.

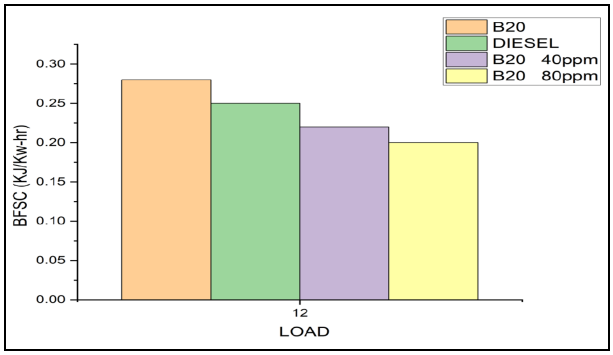


Fig. 6: Variation of BSFC with 12 kg engine load for different fuel blends

5.3 Combustion Graphs

Fig. 7 to 9 show graphs of different cylinder pressure *vs.* loads. In-cylinder pressure in diesel engines is significantly influenced by the combustion characteristics of the fuel. Biodiesel blends typically exhibit lower in-cylinder pressures compared to diesel fuel. This reduction in pressure is attributed to the slower combustion rate of biodiesel, resulting in a less forceful explosion within the cylinder. Consequently, there is an inverse relationship between the percentage of biodiesel in a blend and the resulting in-cylinder pressure. Cylinder pressure increases with engine load. This trend is evident in the graph for both diesel and biodiesel blends. As the engine operates under heavier loads, more fuel is injected and burned, leading to higher in-cylinder pressures.

Cylinder pressure escalates with increasing engine load. Among the tested fuels, the B20+80 ppm biodiesel blend exhibited the most pronounced pressure rise under these conditions. Cylinder pressure intensifies with escalating engine load, peaking at high load conditions. The fuel injection quantity at higher loads directly contributes to the elevated in-cylinder pressure.

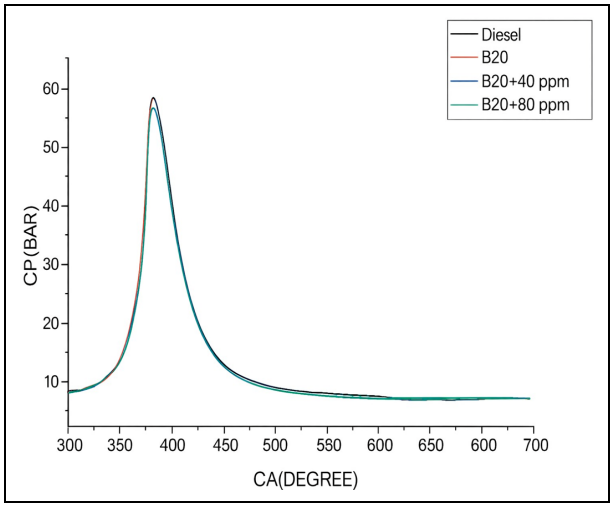


Fig. 7: Cylinder pressure (CP) *vs.* crank angle (CA) for different fuel blends at 3 kg load

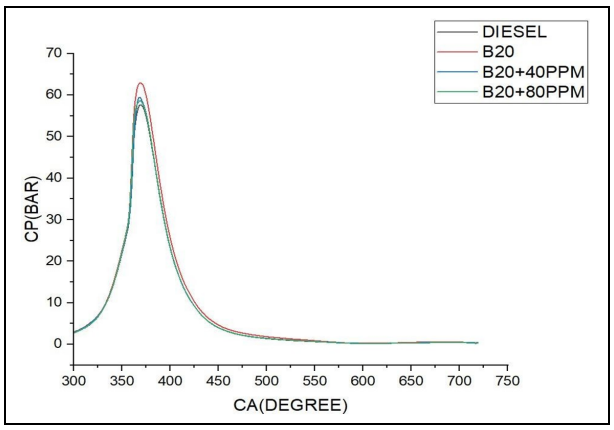


Fig. 8: Cylinder pressure *vs.* crank angle for different fuel blends at 6 kg load

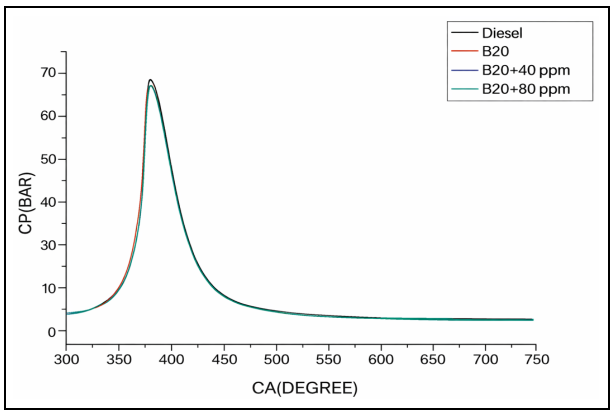


Fig. 9: Cylinder pressure (CP) vs. crank angle (CA) for different fuel blends at 9 kg load

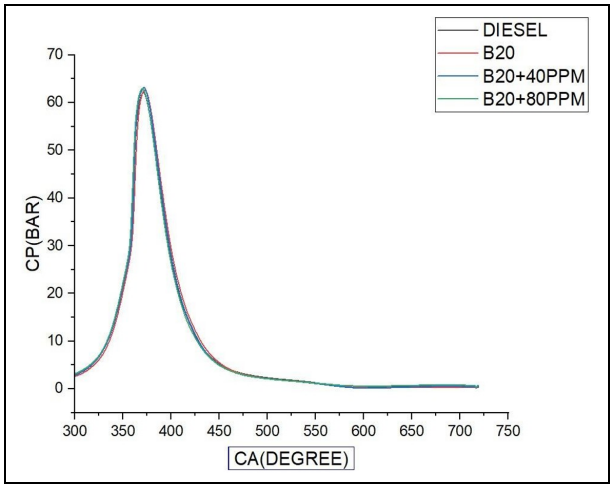


Fig. 10: Cylinder pressure *vs.* crank angle for different fuel blends at 12 kg load

5.4 Net Heat Release Rate

Net Heat Release Rate (NHRR) is a critical parameter that quantifies the rate at which energy is generated during combustion within an engine cylinder. It represents the net energy released by the burning fuel, accounting for heat losses to the cylinder walls and other components. Fig. 10-14 show NHRR at different loads from 3-12 kg.

An increase in engine load resulted in a corresponding advance of the peak heat release point towards Top Dead Center (TDC). Consequently, the rate of heat release intensified under higher load conditions. As engine load increased, the peak heat release point shifted closer to TDC. This shift corresponded to a higher heat release rate. While all fuel blends exhibited this trend, diesel demonstrated a lower heat release rate compared to the B20 blend, indicating variations in combustion characteristics between the two fuels.

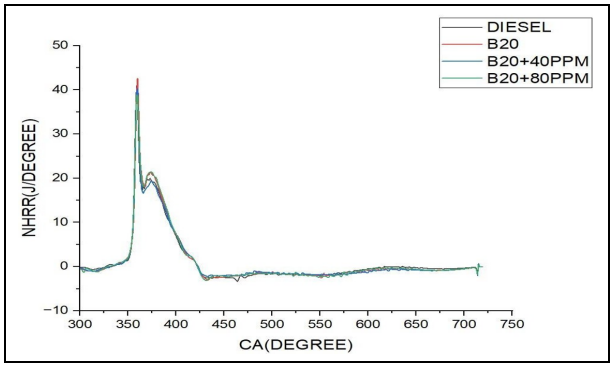


Fig. 11: Net heat release rate (NHRR) *vs.* crank angle for different fuel blends at 3 kg load

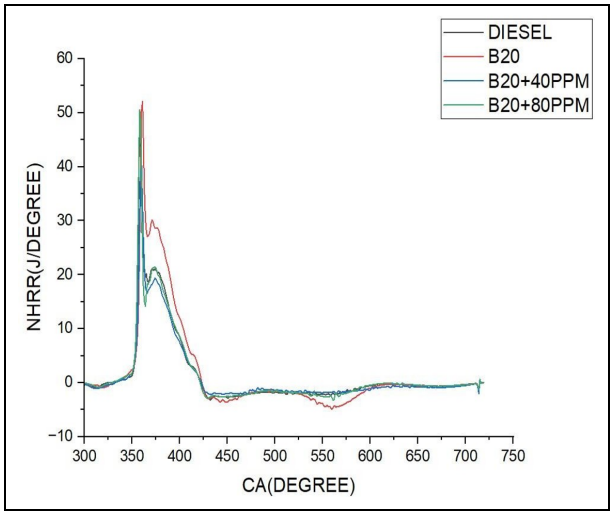


Fig. 12: Net heat release rate *vs.* crank angle for different fuel blends at 6 kg load

As engine load increased, the peak heat release rate advanced towards TDC. This advancement coincided with a higher overall heat release rate. While all fuel blends exhibited this trend, diesel fuel displayed a lower heat release rate compared to the biodiesel blends, indicating distinct combustion characteristics. Under full load conditions, the peak heat release point consistently shifted closer to TDC as engine load increased (Sarma *et al.* 2025). Among the tested fuel

blends, the B20+80 ppm exhibited the highest heat release rate.

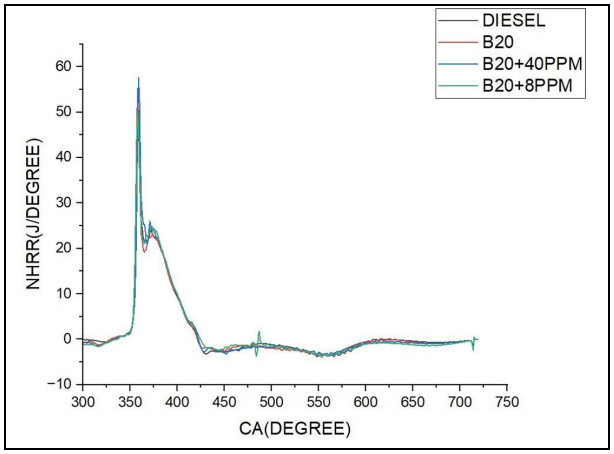


Fig. 13: Net heat release rate *vs.* crank angle for different fuel blends at 9 kg load

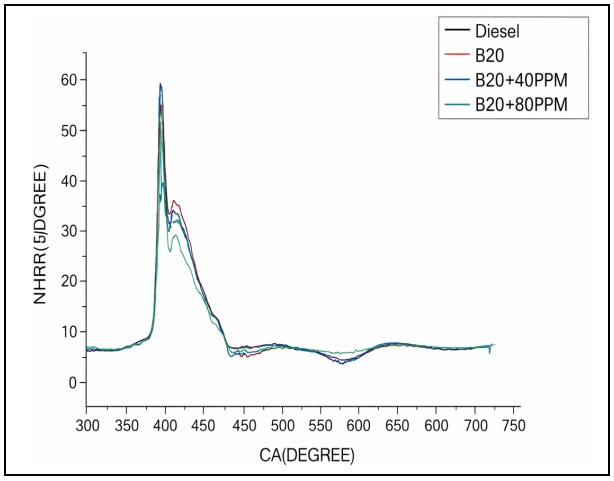


Fig. 14: Net heat release rate *vs.* crank angle for different fuel blends at 12 kg load

5.5 Rate of Pressure Rise (RoPR)

It is a critical parameter in combustion analysis that measures the speed at which pressure increases within the engine cylinder during the combustion process. It provides valuable insights into the combustion characteristics, including ignition delay, combustion phase duration, and the intensity of the burning process.

A high RoPR often indicates rapid and intense combustion, which can lead to engine knock if not managed properly. On the other hand, a low RoPR might suggest slower and less efficient combustion. Fig. 15-18 show RoPR at different loads.

Diesel fuel exhibited a higher RoPR compared to biodiesel blends across all load conditions. This indicates a more rapid combustion process for diesel, influencing overall engine performance and emissions. Biodiesel blends exhibited a lower rate of pressure rise compared to diesel fuel. This slower combustion rate in biodiesel blends is evident across different load conditions. Conversely, diesel fuel demonstrated a higher rate of pressure rise, contributing to improved engine efficiency.

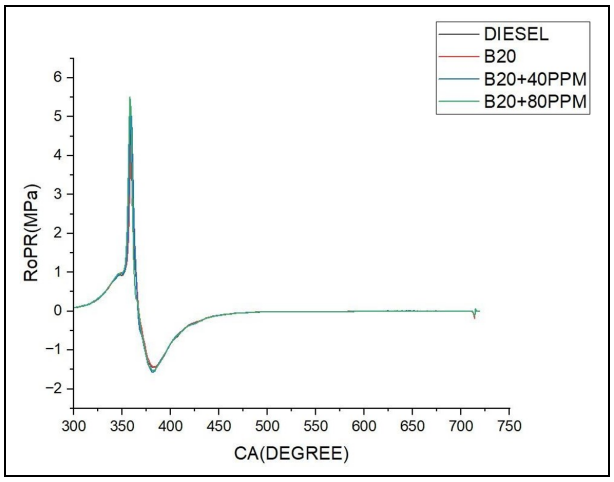


Fig. 15: Rate of pressure rise (RoPR) *vs.* crank angle for different fuel blends at 3 kg load

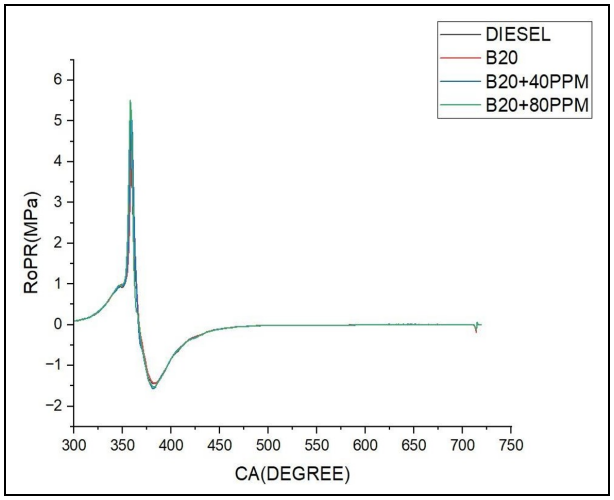


Fig. 16: Rate of pressure rise (RoPR) *vs.* crank angle for different fuel blends at 6 kg load

Biodiesel blends exhibited a lower rate of pressure rise compared to diesel fuel. This indicates a slower and less intense combustion process for biodiesel blends. Conversely, diesel fuel demonstrated a higher rate of pressure rise, contributing to its generally higher engine efficiency. The B20+80 ppm blend displayed the lowest rate of pressure rise among all tested fuels.

At maximum load, diesel fuel exhibited the highest rate of pressure rise. This elevated peak pressure is attributed to the diesel fuel's shorter ignition delay, leading to a more rapid and intense combustion process compared to biodiesel blends.

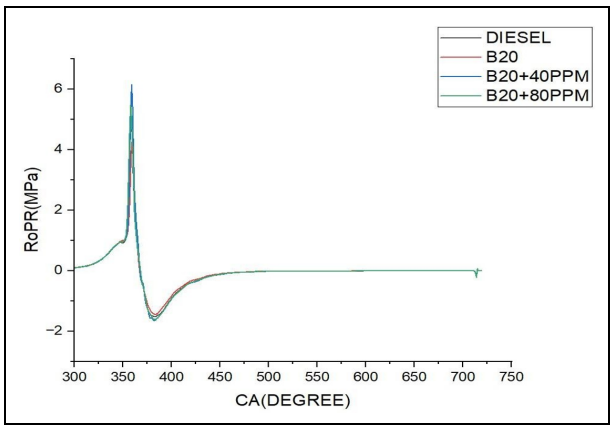


Fig. 17: Rate of pressure rise *vs.* crank angle for different fuel blends at 9 kg load

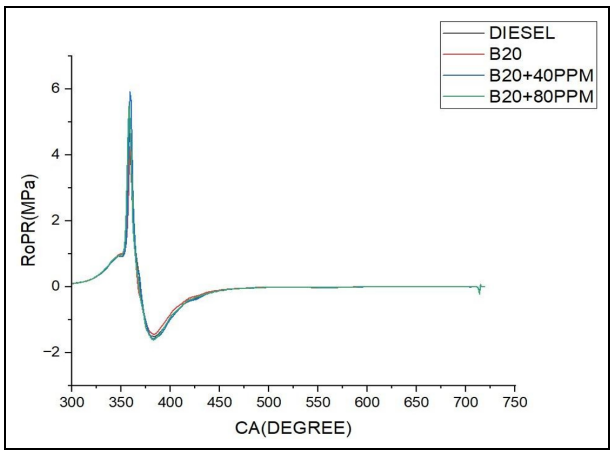


Fig. 18: Rate of pressure rise *vs.* crank angle for different fuel blends at 12 kg load

5.6 Comparison of Maximum Cylinder Pressure (CP) at Full Load

A comparative analysis of maximum cylinder pressure (CP) was conducted for diesel and biodiesel blends under full load conditions. Diesel fuel exhibited the highest peak CP value, indicating a more rapid and intense combustion process. The biodiesel blends, particularly B20+80 ppm, demonstrated lower peak CP values, suggesting efficient combustion compared to diesel.

Fig. 19 shows the overall trend of an engine. As engine load increases, the maximum cylinder pressure (CP MAX) generally increases for all fuel types. This is a typical trend observed in internal combustion engines as more fuel is injected and burned at higher loads.

Diesel fuel consistently exhibits the highest CP MAX values across all load ranges. Biodiesel blends show lower CP MAX values compared to diesel. This suggests a less intense combustion process for biodiesel blends. The addition of nanoparticles (B20+40 ppm and B20+80 ppm) to the B20 blend appears to have a minimal impact on CP MAX, with the curves closely following the B20 curve.

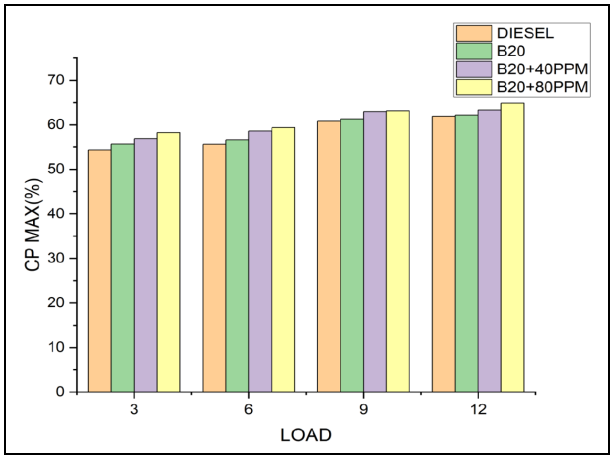


Fig. 19: Maximum cylinder pressure *vs.* engine load for different fuel blends

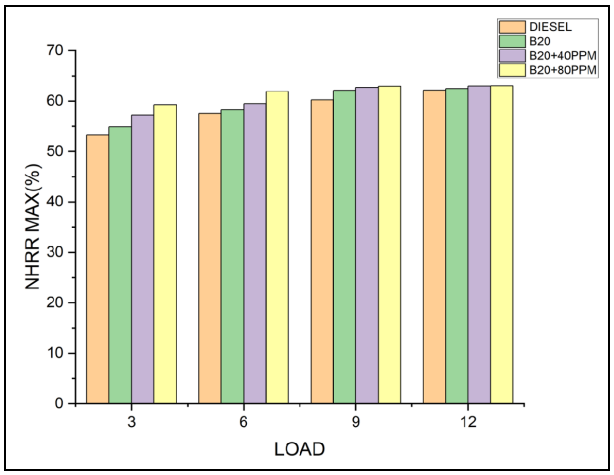


Fig. 20: Maximum net heat release Rate *vs.* engine load for different fuel blends

5.7 Comparison of Maximum Net Heat Release Rate (NHRR) at Full Load

A comparative analysis of maximum NHRR was conducted for diesel and biodiesel blends under full load conditions (Fig. 20). Diesel fuel exhibited the highest peak NHRR value, indicating a more rapid and intense combustion process. The biodiesel blends, particularly B20+80 ppm, demonstrated lower peak NHRR values, suggesting efficient combustion compared to diesel.

Diesel consistently exhibits the highest NHRR MAX values across all load ranges. Biodiesel blends show lower NHRR MAX values compared to diesel. This suggests a less intense combustion process for biodiesel blends. The addition of nanoparticles to the B20 blend appears to have a minimal impact on NHRR MAX, with the curves closely following the B20 curve.

5.8 Rate of Pressure Rise Peak Value

As engine load increases, the RoPR MAX generally decreases for all fuel types. This indicates a slower and less intense combustion process at higher loads (Fig. 21).

Diesel exhibits the highest RoPR MAX values across all load ranges, suggesting a more rapid and intense combustion process. Biodiesel blends show lower RoPR MAX values compared to diesel, indicating a slower combustion process. The addition of nanoparticles seems to have a limited impact on RoPR MAX, with the curves for B20+40 ppm and B20+80 ppm closely resembling the B20 curve.

The graph suggests that diesel fuel tends to generate higher rates of pressure rise compared to biodiesel blends. This is likely due to the higher energy content and combustion characteristics of diesel. The addition of nanoparticles in this case does not seem to significantly influence the maximum RoPR.

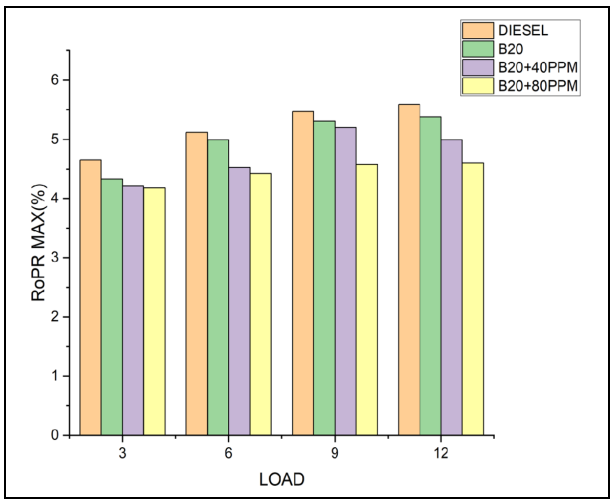


Fig. 21: Rate of pressure rise *vs.* engine load for different fuel blends

7. CONCLUSION

The study investigated the impact of $CuCl_2$ nanoparticles on the performance and emission characteristics of a diesel engine operating on a B20 biodiesel blend. The addition of $CuCl_2$ nanoparticles with the dispersant B20 blend improved BTE and reduced BSFC. Emissions of carbon monoxide, unburnt hydrocarbons, nitrogen oxides, and smoke were significantly lower with the nanoparticle-treated fuel.

At the maximum load, the B20+40 ppm $CuCl_2$+dispersant blend exhibited an 8.28% increase in BTE and a 1.42% decrease in BSFC. Similarly, the B20+80 ppm blend showed a 5.06% increase in BTE and a 0.91% decrease in BSFC. Emissions reductions were substantial, with B20+40 ppm $CuCl_2$+dispersant showing decreases of 65.7% in CO, 22.7% in UHC, 40.37% in NO_x, and 15.5% in smoke. The B20+80 ppm blend demonstrated similar reductions, with decreases of 57.1% in CO, 24.5% in UHC, 39.08% in NO_x, and 10.07% in smoke.

FUNDING

This research received no specific grant from any funding agency in the public, commercial, or not-for-profit sectors.

CONFLICTS OF INTEREST

The authors declare that there is no conflict of interest.

COPYRIGHT

This article is an open-access article distributed under the terms and conditions of the Creative Commons Attribution (CC BY) license (http://creativecommons.org/licenses/by/4.0/).

REFERENCES

Dueso, C., Muñoz, M., Moreno, F., Arroyo, J., Gil-Lalaguna, N., Bautista, A., Gonzalo, A. and Sánchez, J. L., Performance and emissions of a diesel engine using sunflower biodiesel with a renewable antioxidant additive from bio-oil, *Fuel*, 234, 276-285 (2018). https://doi.org/10.1016/j.fuel.2018.07.013

Erkan, O., Performance, emissions, combustion and injection characteristics of a diesel engine fuelled with canola-oil-hezelnut soapstock biodiesel mixture, *Fuel Process. Tech.*, 129(5), 183-191 (2015). http://dx.doi.org/10.1016/j.fuproc.2014.09.016

Habibullah, M., Masjuki, H. H., Kalam, M. A., Fattah, I. M. R., Ashraful, A. M. and Mobarak, H. M., Biodiesel production and performance evaluation of coconut, palm and their combined blend with diesel in a single-cylinder diesel engine, *Energy Convers. Manag.*, 87, 250-257 (2014). https://doi.org/10.1016/j.enconman.2014.07.006

Junshuai, L., Su, W. and Beibei, M., The effects of nano-additives added to diesel-biodiesel fuel blends on combustion and emission characteristics of diesel engine: a review, *Energies*, 15 (3), 1032 (2022). https://doi.org/10.3390/en15031032

Kalam, M. A., Husnawan, H. H. and Masjuki, H. H., Exhaust emission and combustion evaluation of coconut oil-powered indirect injection diesel engine, *Renew. Energy*, 28(15), 2405-2415 (2003). https://doi.org/10.1016/S0960-1481(03)00136-8

Machacon, H. T. C., Matsumoto, Y., Ohkawara, C., Shiga, S., Karasawa, T. and Nakamura, H., The effect of coconut oil and diesel fuel blends on diesel engine performance and exhaust emissions, *JSAE Rev*., 22 (3), 349-355 (2001a). https://doi.org/10.1016/S0389-4304(01)00111-4

Machacon, H., Shiga, S., Karasawa, T. and Nakamura, H., Performance and emission characteristics of a diesel engine fueled with coconut oil-diesel fuel blend, *Biomass Bioenergy*, 20(1), 63-69 (2001b). https://doi.org/10.1016/S0961-9534(00)00059-3

Manzoore, E. M. S., Nik, N. N. G., Kalam, M. A., Irfan, A. B., Banapurmath, N. R., Ali, M. A. B., Kamangar, S., Cho, H. M. and Akram, N., An investigation on the influence of aluminium oxide nano-additive and honge oil methyl ester on engine performance, combustion and emission characteristics, *Renew. Energy*, 146, 2291–2307 (2020). https://doi.org/10.1016/j.renene.2019.08.025

Manzoore, E. M. S., Nik, N. N. G., Md, A. K., Badruddin, I. A., Banapurmath, N. R. and Naveed, A., The effect of nano-additives in diesel-biodiesel fuel blends: a comprehensive review on stability, engine performance and emission characteristics, *Energy Convers. Manage.*, 178, 146–177 (2018). https://doi.org/10.1016/j.enconman.2018.10.019

Mofijur, M., Rasul, M. G. and Hyde, J., Recent developments on internal combustion engine performance and emissions fuelled with biodiesel-diesel ethanol blends, *Procedia Eng.*, 105, 658–664 (2015). http://dx.doi.org/10.1016/j.proeng.2015.05.045

Mohadesi, M., Hojabri, Z. and Moradi, G., Biodiesel production using alkali earth metal oxides catalysts synthesized by sol-gel method, *Biofuel Res. J*., 1 (1), 30–33 (2014).

Munimathan, A., Rajendran, S., Tripathi, A. K., Jayabalan, J., Palanivel, V., Varma, R., Prabhakar, S., & Alwetaishi, M., ML techniques increasing the power factor of a compression ignition engine that is powered by Annona biodiesel using SATACOM, *Scientific Rep.*, 15(1), 11669(2025). https://doi.org/10.1038/s41598-025-91162-1

Patil, P. D. and Deng, S., Optimization of biodiesel production from edible and non-edible vegetable oils, *Fuel,* 88(7), 1302-1306 (2009). https://doi.org/10.1016/j.fuel.2009.01.016

Sabri, A. M., Talib, N., Sani, A. S. A. and Kunar, S., Investigation on the performance of modified vegetable oil lubricants with single and hybrid nanoparticle additives for MQL applications, *Tribol. Int.*, 214, 111314 (2026). https://doi.org/10.1016/j.triboint.2025.111314

Sarma, C. J., Medhi, B. J., Bora, B. J., Bora, D. K., Elumalai, P. V., Lawrence, K. R., Barik, D., Ramegowda, R., Kavalli, K., Soudagar, M. E. M. and Altaye, M. D., Analysis of the pooled effect of compression ratio and injection timing variation on conventional diesel engine powered with nano doped biodiesel blend, *Sci. Rep*., 15(1), 21209(2025). https://doi.org/10.1038/s41598-025-98510-1

Tao, C., Dan, Z., Yuze, S., Siliang, N., Li, W., Di, G. and Bing, W., Evaluation of NO_x emissions characteristics in a CO2-Free micro-power system by implementing a perforated plate, *Renew. Sustain. Energy Rev*., 145, 111150 (2021). https://doi.org/10.1016/j.rser.2021.111150

Venkatesan, H., Sivamani, S., Sampath, S., Gopi, V. and Dinesh, K. M., A comprehensive review on the effect of nano metallic additives on fuel properties, engine performance and emission characteristics, *Int. J. Renew. Energy Res.*, 7(2), 825–843 (2017). https://doi.org/10.20508/ijrer.v7i2.5678.g7064

Zhang, H., Prabhahar, M., Prakash, S., Karpaga, V. B. and Dhanraj, T., Investigating the impact of oxygenated additives (DEE, DME &MTBE) on engine performance and emission reductions in simarouba methyl ester blends, *Int. Res. J. Multidisc. Tech.,*7(3), 112–123(2025). https://doi.org/10.54392/irjmt25310